

A measurement of the $^{12}\text{C}(n,2n)$ cross section from threshold to 26 MeV

Keith Mann, Tyler Reynolds, and Mark Yuly, Houghton College

Introduction

An experiment to measure the cross section for the $^{12}\text{C}(n,2n)$ reaction in the energy range of the tertiary neutrons produced by inertial confinement fusion has been performed using the 4.5 MV Tandem Van de Graaff accelerator at the Ohio University Accelerator Laboratory. This reaction, with a threshold of 20.295 MeV, may be useful as a diagnostic tool for measuring the flux of tertiary neutrons, since it is insensitive to the large number of 14 MeV primary neutrons produced in the primary DT fusion reaction. Graphite disks placed within the ICF reaction chamber would be activated by the tertiary neutrons and yet able to survive even in the harsh environment once ignition is achieved.

In this experiment, monoenergetic neutrons produced using the $^3\text{H}(d,n)^4\text{He}$ reaction were allowed to strike carbon-containing targets of polyethylene and graphite. When these neutrons induced the $^{12}\text{C}(n,2n)^{11}\text{C}$ reaction, ^{11}C nuclei were produced, which later decayed via β^+ emission with a half-life of about 20 minutes. After an activation period, the targets were removed to counting stations, where the rate of back-to-back gamma rays resulting from positron annihilation was used to determine the number of ^{11}C nuclei present. In order to determine the neutron flux, protons from neutron-proton elastic scattering were simultaneously counted in a ΔE -E detector telescope. Figure 1 shows the preliminary results of this experiment. While further work will be required before the absolute $^{12}\text{C}(n,2n)$ cross section can be determined, the preliminary analysis is encouraging. The measured cross sections are of the correct order of magnitude, have the predicted increasing trend with incident neutron energy, and the threshold is where it was expected.

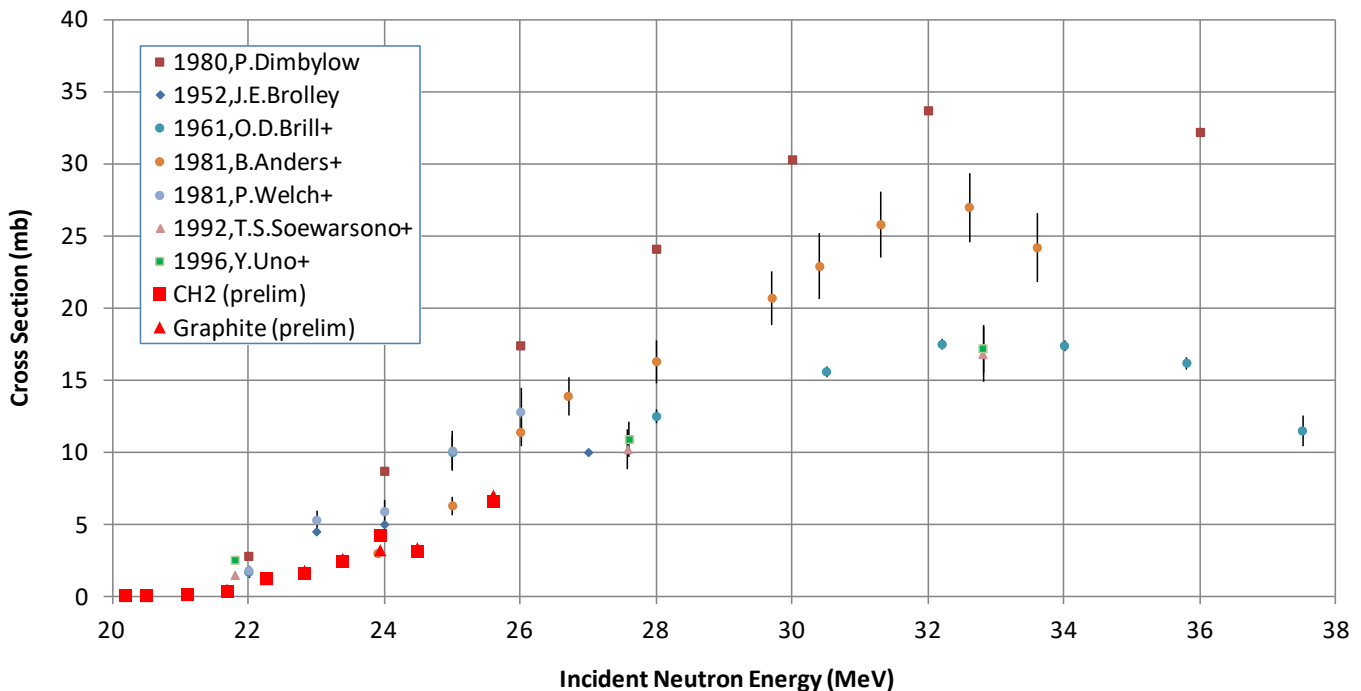


Figure 1. Previous and current experimentally measured and calculated cross sections for $^{12}\text{C}(n,2n)$. Very preliminary results for the present measurement using the polyethylene target (red squares) and graphite target (red triangles) are shown. Statistical error bars are smaller than symbols for current measurements.

Previous measurements

In order to use this technique to measure the production of tertiary ICF neutrons, accurate cross sections are needed. Figure 1 also shows the measurements that have been made to date for this reaction in the energy range between 20 and 38 MeV. The cross sections from P. Dimbylow [1] are from a nuclear model calculation using fits to experimentally measured total, elastic and inelastic cross sections. It is observed that the experimental cross sections tend to follow two separate curves, differing by as much as a factor of two. The two curves span the entire range of neutron energies of interest, with the data points in the upper curve mostly from B. Anders et al. [2] but also P. Welch et al. [3]. The lower curve is mostly the measurements from O. D. Brill et al. [4], Soewarsono et al [5], and Uno et al. [6] Even near threshold, where the measured cross section curves converge, the cross sections still do not agree.

It is difficult to see what might be causing the results for these experiments to fall into two distinct curves. Table 1 summarizes, as much as possible from the published descriptions, the essential features of each previous experiment. The experiments that are highlighted in gray gave results falling on the upper curve; the others tend to lie near the lower curve. There does not seem to be any obvious division between the experiments on the basis of technique, type of neutron source, type of target, method of neutron flux determination or type of activation measurement.

Table 1. Previous measurements of the $^{12}\text{C}(n,2n)$ cross section in the energy range 20-30 MeV.

Year	Experimenters	Accelerator	Neutron source	Target	Neutron Flux measurement	Activation measurement
1952	Brolley, Fowler, Schlacks [7]	10.5 MeV deuterons from cyclotron	$^3\text{H}(d,n)$ gas cell, neutron energy selected by angle	polyethylene (CH_2) foils, 11 mg/cm ²	Calculated using $^3\text{H}(d,n)$ cross section	Calibrated end-window Geiger counters to detect ^{11}C decay positrons
1961	Brill et al. [4]	20 MeV deuterons from cyclotron, slowed down by Pt foils (0.7 MeV resolution)	$^3\text{H}(d,n)$ and $^2\text{H}(d,n)$, T+Zr solid and gas ^2H target	Teflon, CF_2	Energy/angle distribution measured using neutron TOF. Claims measured +/- 30%	Counted β^+ annihilation gammas in Geiger counter, compared to ^{197}Au .
1980	Dimbylow [1]	Nuclear model calculation, statistical level density model based on optical model fits to experimental total, elastic and inelastic cross sections.				
1981	Anders, Herges, Scobel [2]	7-16 MeV deuterons from cyclotron, degraded to 5.7-9.2 MeV by Be foil	$^3\text{H}(d,n)$ Titanium foil, 10 μm thick, adsorbed tritium	cylindrical (22 mm diam), reactor graphite	Recoil proton detector (stilbene crystal at 0 deg). Neutron monitor to correct for fluctuations in flux.	Annihilation gamma-gamma coincidence using 2 NaI detectors
1981	Welch et al. [3]	Ohio University Tandem	$^3\text{H}(d,n)$	Natural sample, 1.77 cm-diameter by 1.0 cm thick	No information available.	Ge(Li) Detector calibrated with NaCl sample.
1992	Soewarsono et al. [5]	20-40 MeV protons from cyclotron.	$^7\text{Li}(p,n)$ quasimonoenergetic; lithium on graphite backing, background subtracted.	Natural sample	Neutron TOF to NE-213 liquid scintillator detector, see Uno et al.	Single HPGe detector, Activate with Li target and no Li target and subtract
1996	Uno et al. [6]	20-40 MeV protons from cyclotron.	$^7\text{Li}(p,n)$ quasi-monoenergetic, width varies 2.3-1.4 MeV for 18-40 MeV neutrons, respectively.	Cylindrical (20 mm diam), graphite	Activation of Li target gave absolute normalization, neutron time of flight measured angular and energy distribution.	Two HPGe detectors detected decay gammas, no coincidence required.

Although it is not clear why they disagree, the previous experiments had several weaknesses that were addressed in the current measurement. One difficulty encountered in all of the experiments was to ascertain the incident neutron flux and its energy dependence. This was particularly important for the experiments using the ${}^7\text{Li}(p,n)$ reaction to produce the neutrons, since there was a significant contribution from unwanted lower energy neutrons. Many of the cyclotron experiments also suffered from a relatively broad neutron energy distribution. Earlier experiments used stilbene or liquid scintillators, which have limited energy resolution and particle identification capability, to detect neutrons or recoiling protons. Several of them used TOF techniques which, while ideal for measuring the neutron energy spectrum, had trouble giving the absolute flux.

By instead using a recoil proton telescope with ΔE -E silicon detectors, the current experiment has the advantage of excellent proton energy resolution as well as the ability to identify and select only recoil protons of the correct energy. Since the solid angle is well defined and the efficiency is nearly 100% for these detectors, an absolute measurement becomes much easier. Two targets, graphite and polyethylene, irradiated and counted simultaneously, allow a consistency check. Moreover, since the polyethylene activation target is also the converter for the proton telescope, corrections that result from the neutron flux being measured in a different place than the activation target are reduced.

Experiment

The ${}^{12}\text{C}(n,2n)$ cross sections were measured for energies between about 20 and 26 MeV using the 4.5 MV Tandem van de Graaff accelerator at Ohio University. Figure 2 shows a schematic diagram of the activation set up. Deuterons were accelerated to energies between 3.5 and 8.285 MeV and allowed to strike a titanium tritide foil with a nominal $3.3\ \mu\text{Ci}$ activity. Beam currents were typically between 0.5 and $1.0\ \mu\text{A}$. The titanium was deposited on a 0.254 mm thick copper substrate of 2.54 cm diameter, which was located in the end of the beam pipe, just upstream of an aluminum end window. The end window was cooled by a stream of air. The end of the beam line, including the target, was moved in a circular path by the “wobbler” to keep the beam from overheating any one place on the target. Before striking the target, the deuteron beam was defocused by a pair of quadrupole magnets located 275 and 315 cm upstream, and allowed to pass through a 1.27 cm diameter collimator 45 cm upstream of the target. This was to ensure that the beam spot striking the target was relatively large to reduce heating, and that it always struck the target at the same known location.

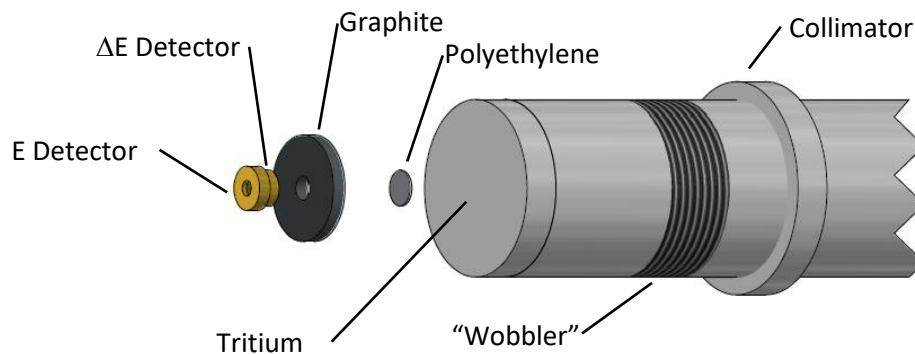


Figure 2. The experimental setup for activating targets. Deuterons travelling down the beam pipe were collimated, then struck the tritium target to produce neutrons. These neutrons activated the graphite and polyethylene targets via the ${}^{12}\text{C}(n,2n)$ reaction. The polyethylene target also acted as the converter for the recoil proton telescope. The recoiling protons were identified and counted using a ΔE -E detector. The “wobbler” moved the end of the beam pipe carrying the tritium target to keep it from overheating.

An aluminum target and detector holder, shown in Figure 3a, was used to position the polyethylene and graphite targets, and to hold the detectors in fixed positions at an angle of 0° with respect to the beam. Neutrons leaving the neutron source were allowed to strike a 1.64 mm thick, 2.54 cm diameter high-density polyethylene target located 6.5 cm from the tritium target. Located 14.5 cm downstream of the polyethylene was a 7.62 cm diameter 0.89 cm thick disc of high purity graphite, with a 17.46 mm hole drilled in through its center. Upstream of the graphite target were a pair of shields used to stop protons scattered from the polyethylene from reaching the graphite target. The two shields, one 1.28 mm and the other 2.57 mm thick, were graphite disks of the same cross section as the graphite target.

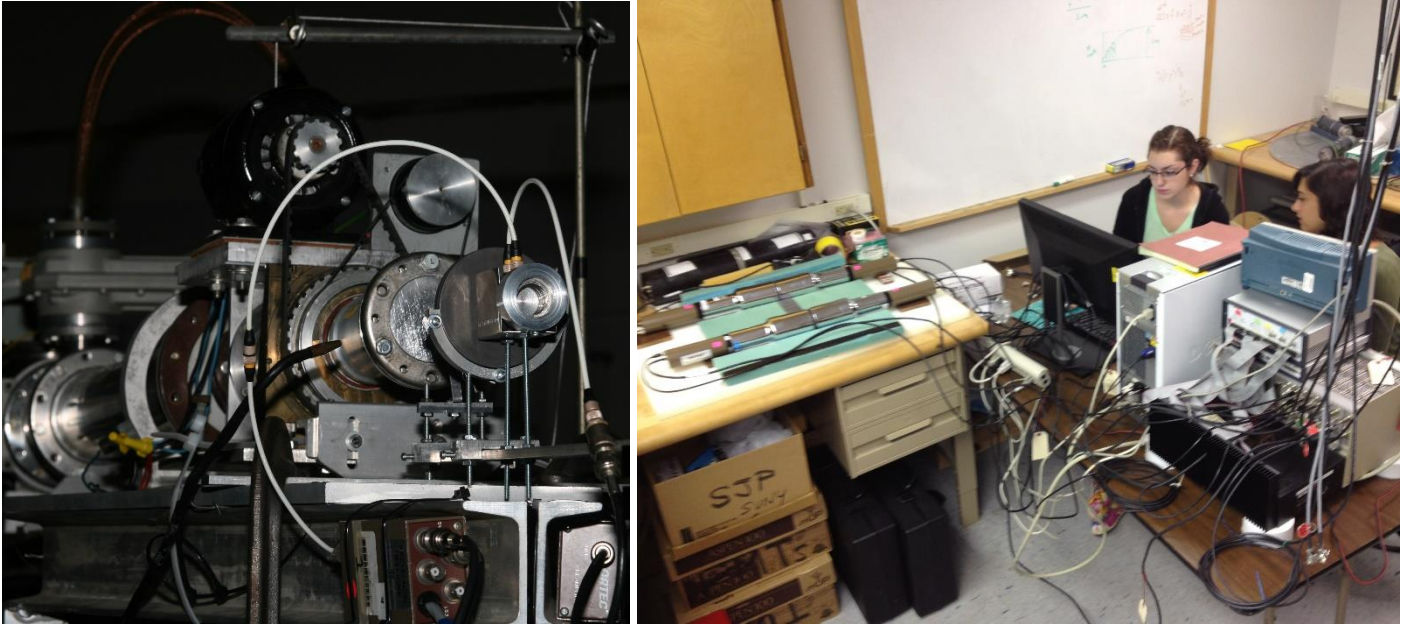


Figure 3.(a) (left) A photograph of the activation setup showing the targets and detectors and their support stands. (b) (right) Three counting stations were used for the graphite target, the polyethylene target, and the graphite shields.

A proton telescope consisting of a $300\ \mu\text{m}$ thick, $150\ \text{mm}^2$ ion implanted silicon ΔE detector and a $2000\ \mu\text{m}$ thick, $100\ \text{mm}^2$ silicon surface barrier E detector was placed behind the hole in the graphite target, so that protons coming from the polyethylene could be viewed. The entrance of the ΔE detector was covered by a $0.005\ \text{mm}$ thick aluminum foil to keep out ambient light. In between the detectors, 18.5 cm from the tritium target, a tantalum collimator consisting of four washers defined the entrance aperture for the telescope. The collimator was 1.0 mm thick with a 9.54 mm diameter hole. The entire detector assembly was housed in an aluminum tube with wall thickness of about 8.7 mm and diameter of 3.18 cm. Preamplifiers and spectroscopy amplifiers located near the detectors in the experimental hall sent pulses to a FastComTech MPA-4 multiparameter system which digitized and recorded the pulse heights and timing. As seen in Figure 4, from this a 2D histogram of the pulse height in the dE detector versus the pulse height in the E detector was made, which allowed clear identification of the protons of interest.

In addition to the proton telescope pulse heights and timing, the system also recorded the integrated deuteron beam current and information from the neutron monitor. The neutron monitor was a 5 inch diameter liquid scintillator detector located approximately 750 cm from the tritium target at an angle of a few degrees to beam right. In order to identify neutron pulses from gammas, a pulse shape analysis was performed and the pulse height and rise time recorded by the MPA-4 system.

Activated targets were counted at three counting stations located in an adjacent room, shown in Figure 3b. After each was activated simultaneously, the graphite and polyethylene targets were placed between pairs of 3 inch diameter by 3 inch thick NaI detectors. Coincidence events consisting of two back-to-back 0.511 keV gamma rays from positron annihilation could be selected and counted as a function of time. This allowed the growth curve of ^{11}B to be measured and fit in order to determine the number of ^{11}C nuclei present. The gamma rays from the graphite shields were counted in a separate station consisting of two HPGe detectors in order to look for activation due to contaminants in the graphite. Pulses from all of these detectors were sent to a FastComTech MPA-3 system, which recorded the pulse heights and timing information.

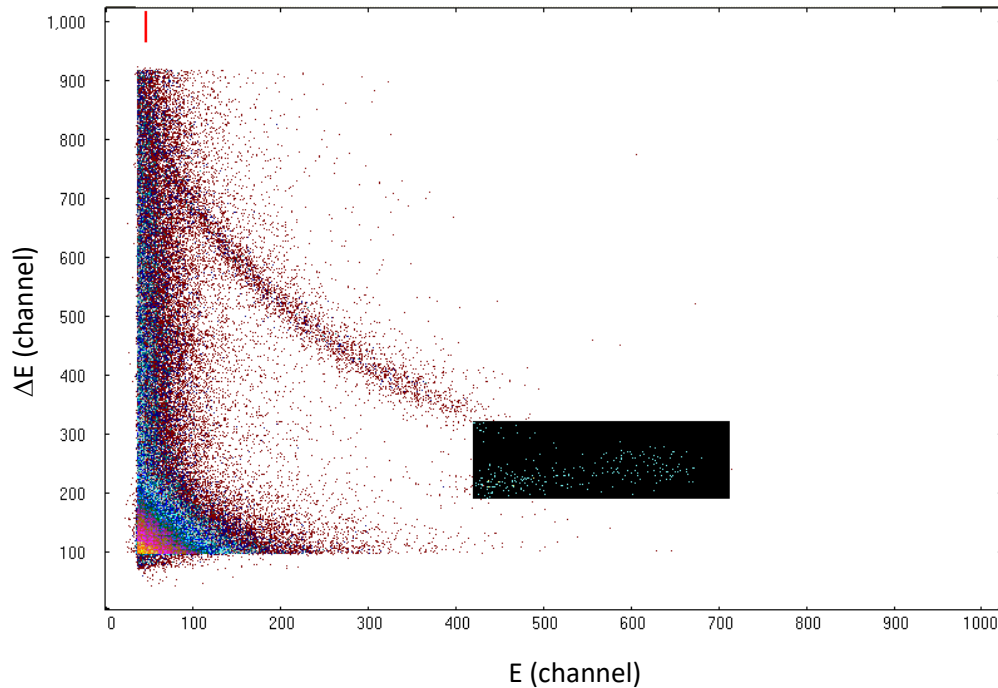


Figure 4. A plot of ΔE versus E for 24.5 MeV neutrons striking the polyethylene target. The proton band is clearly visible. The marked region-of-interest indicates the protons counted as elastically scattered by neutrons.

Procedure

Prior to the experiment at Ohio University, the proton telescope was tested using the 3.4 MeV Pelletron accelerator at SUNY-Geneseo. Protons with energies of approximately 22.5 MeV were created using the $\text{D}(^3\text{He},\text{p})$ reaction by allowing a ^3He beam to strike a 3.7 μm thick deuterated polyethylene target. The protons traveled through 13 μm thick kapton window followed by 10 cm of air and an aluminum degrader before entering the detector. In the degraders of thicknesses of 0.00, 0.91, 1.27, 2.18 mm the protons lost energy, and upon entering the detector telescope had energies of 22.213, 17.282, 15.032, and 7.306 MeV respectively. A numerical model was created which allowed the proton energy loss in each detector to be calibrated prior to taking the detector to Ohio University. Figure 5, which plots the energy lost in the ΔE detector versus the energy in the E detector, reveals a very clear proton band which agrees well with the calculated band.

Once at Ohio University, the detector and targets were first aligned with the beam line using a laser. The laser tripod was placed directly above a beam line monument on the floor, approximately 6 m from the tritium target, and leveled with a bubble level. It was then adjusted to hit another beam line marker on the wall where the beam entered the experimental hall and a plumb line directly over the collimator. The laser height was adjusted to 175.2 cm, the approximate beam height. Once the laser was travelling along the beam path, it was used to position the targets and detectors.

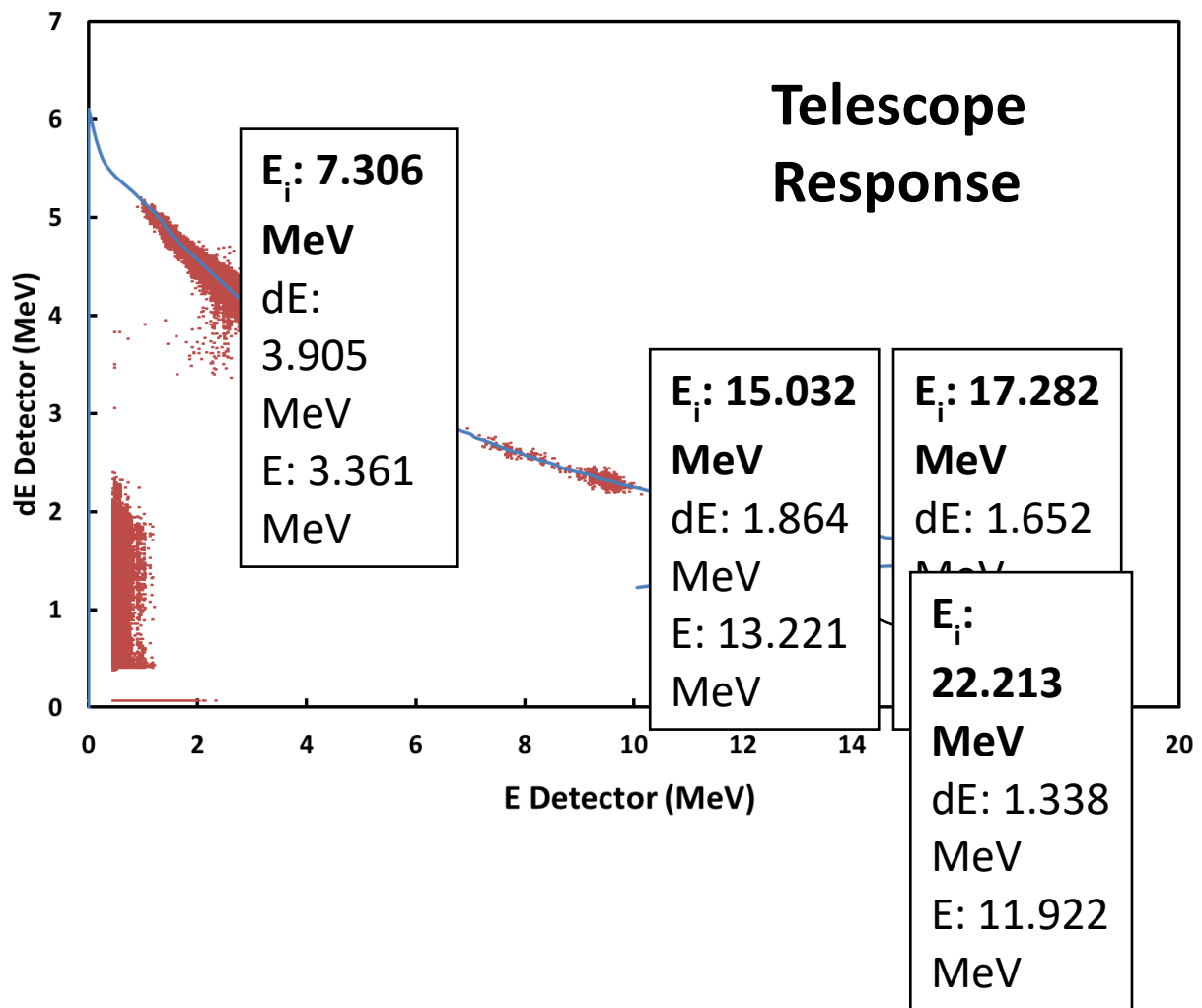


Figure 5. Energy calibration of the ΔE -E telescope. The blue curve represents the calculated energy loss for protons in the ΔE and E detectors. The 22.5 MeV protons (red dots) from the ${}^2\text{H}({}^3\text{He},\text{p})$ reaction were slowed down in air and aluminum energy degraders to give proton energies of 22.213, 17.282, 15.032 and 7.306 MeV. Labels show the location of these protons along the calculated proton band.

For each energy setting, prior to activating the targets a study was made of the positioning of the beam in the beam pipe. This is important because a small change in the position of the beam spot on the tritium target had a large effect on the scattering angles and therefore the count rates. In order to ensure proper alignment of the beam, the current in the last quadrupole magnet just before the collimator was changed. Any displacement from the central axis of the beam pipe would then cause the beam spot to move, which could be detected by carefully monitoring the number of protons per integrated charge and the ratio of protons to neutrons detected in the neutron monitor. When these diagnostics did not change with quadrupole setting the beam was assumed to be centered in the beam pipe.

Following the quadrupole tests, a graphite target and a polyethylene target were placed in the target holders to be activated for about 1.5 hours. Three identical sets of targets were available to be used consecutively in order to allow enough time for any longer lived activated contaminants to decay, although none were detected using the germanium detectors. When the deuteron beam was stopped, after sufficient time to allow the radiation dose rate to fall to an acceptable level, the targets were hand-carried to the counting room and placed in the counting stations. The time between when irradiation stopped and when target counting commenced was

recorded, and was typically around 4-5 minutes. Each sample was then counted for approximately 1.5 hours, with the rate binned into one minute intervals.

The number of background protons was measured at each energy setting by removing the polyethylene target and counting for approximately 30 minutes. A special graphite disk and shield set was used exclusively for this purpose; however, for some energy settings the hole in the center of the graphite discs used for background measurements was 14.29 mm in diameter. Towards the end of the experiment this was increased to 17.46 mm to match the discs which were activated.

Analysis

The preliminary cross sections, which are shown in Figure 1, were determined directly from the number of ^{11}C nuclei created by activation of the natural graphite target and the neutron flux determined from np elastic scattering of protons into the proton telescope using some simplifying assumptions.

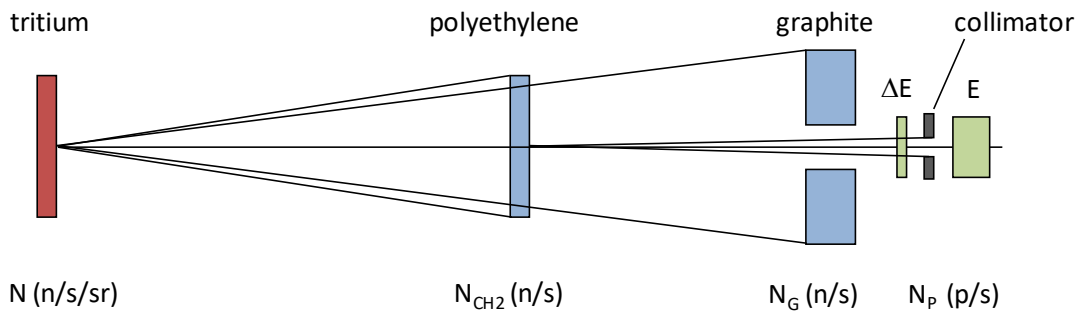


Figure 6. A schematic diagram used for initial estimates of the cross section. The tritium and polyethylene targets are treated as point sources for neutrons and protons, respectively.

To see how the neutron flux was approximately calculated, consider the diagram in Figure 6. Assume that the tritium target is an isotropic point source of monoenergetic neutrons with flux N (neutrons/sec/sr). In that case, the number/sec of neutrons on the polyethylene (N_{CH_2}) and graphite (N_{G}) targets would be given by

$$N_{\text{CH}_2} = N \Omega_{\text{CH}_2} \quad \text{and} \quad N_{\text{G}} = N \Omega_{\text{G}} \quad (1)$$

where Ω_{CH_2} and Ω_{G} are the solid angles of the plastic and graphite targets, respectively, if the effect of the finite thickness of the targets on solid angle is neglected. The number of protons/sec (N_{P}) detected by the proton telescope can be obtained if the polyethylene target is treated as a point source for the purpose of scattering protons into the proton telescope. Assuming that the cross section for np elastic scattering (σ_{np}) is constant over the angles subtended by the targets, and is equal to the cross section at 0° , yields

$$N_{\text{P}} = \sigma_{\text{np}} N_{\text{H}} N_{\text{CH}_2} \Omega_{\text{P}} \quad (2)$$

Where N_{H} is the thickness (in number of hydrogen nuclei/area) of the polyethylene target, and Ω_{P} is the solid angle of the proton telescope defined by the collimator. Equation 2 allows the neutron rate on the plastic target (N_{CH_2}) to be determined from the proton rate (N_{P}) measured by the proton telescope. Using Equation 1 then gives the neutron flux (N).

The targets were taken to the counting stations, and the number of ^{11}C decays in each was counted. The growth curve for ^{11}B from the positron decay of ^{11}C was determined by integrating the number of counts in one minute wide bins. Figure 7 shows an example of a fit of the growth function

$$R(t) = R_0(1 - e^{-\lambda t}) + At + B \quad (3)$$

to the measured ^{11}B growth curve, where R_0 is the final total number of ^{11}C decays detected, λ is the decay constant for ^{11}C , and A and B are background constants. This value was then corrected for the delay time between when the neutron irradiation ended and when decay counting began. Finally, the total number of ^{11}C present when the neutron bombardment ended (N_{C11}) was determined using the detector efficiencies of 12% and 70% for the graphite and polyethylene targets, respectively.

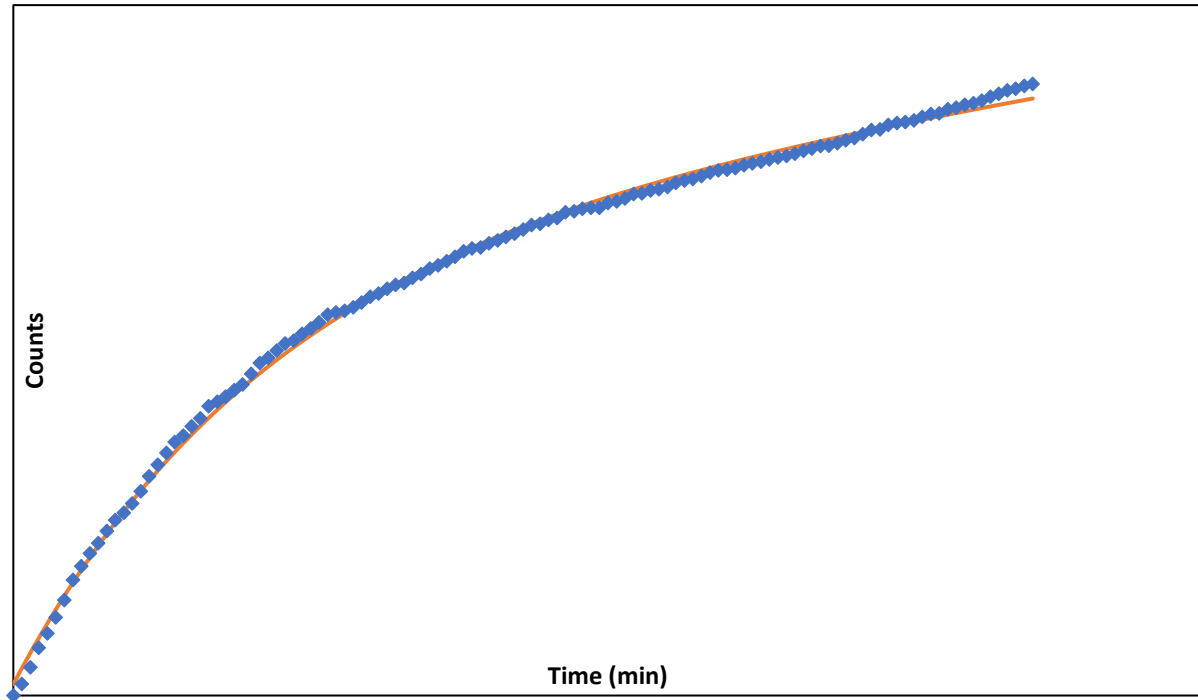


Figure 7. Typical fit to ^{11}B growth curve for the graphite target activated with 23.945 MeV neutrons for about 1.5 hours. This curve was calculated to result from about 27,763 ^{11}C nuclei present when the deuteron beam was turned off.

Now consider the processes occurring in the targets. The number of ^{11}C nuclei is changing, because ^{11}C nuclei are being created by $^{12}\text{C}(n,2n)^{11}\text{C}$ and at the same time ^{11}C nuclei are decaying. The rate the number of ^{11}C nuclei (N_{C11}) changes is given by

$$\frac{dN_{\text{C11}}}{dt} = \sigma N_T N \Omega - \lambda N_{\text{C11}} \quad (4)$$

where $\sigma N_T N \Omega$ is the rate ^{11}C is being created and λN_{C11} is the decay rate. Here σ is the $^{12}\text{C}(n,2n)^{11}\text{C}$ cross section, N_T is the areal density of carbon nuclei in the target, and Ω is the solid angle of the target, either graphite or polyethylene. Solving this differential equation for the cross section yields

$$\sigma = \frac{N_{\text{C11}}}{N_T N \Omega} \frac{\lambda}{(1 - e^{-\lambda t})} \quad (5)$$

These are the cross sections plotted in Figure 1. Clearly, many questionable assumptions were made to arrive at his result, and a more careful analysis needs to be made. In order to determine corrections to the foregoing analysis, a Monte Carlo simulation of our experimental setup has been developed using MCNPX. Figure 1 shows the results of such a simulation, with simulated proton tracks leaving the polyethylene target. The current simulation code allows a realistic extended neutron source to be properly simulated, including the correct flux and neutron energy as a function of angle. The simulation also should properly account for the geometry of the relatively large polyethylene and graphite targets. A correction factor for these effects can be obtained by comparing the ratio N_G/N_P and N_{CH_2}/N_P as calculated in the simulation with the same ratios obtained from Equations 1 and 2. At the present time only a low reliability simulation has been performed, giving a preliminary result that the correction factor for these effects should be about 0.7, that is, the correction is on the order of 30%.

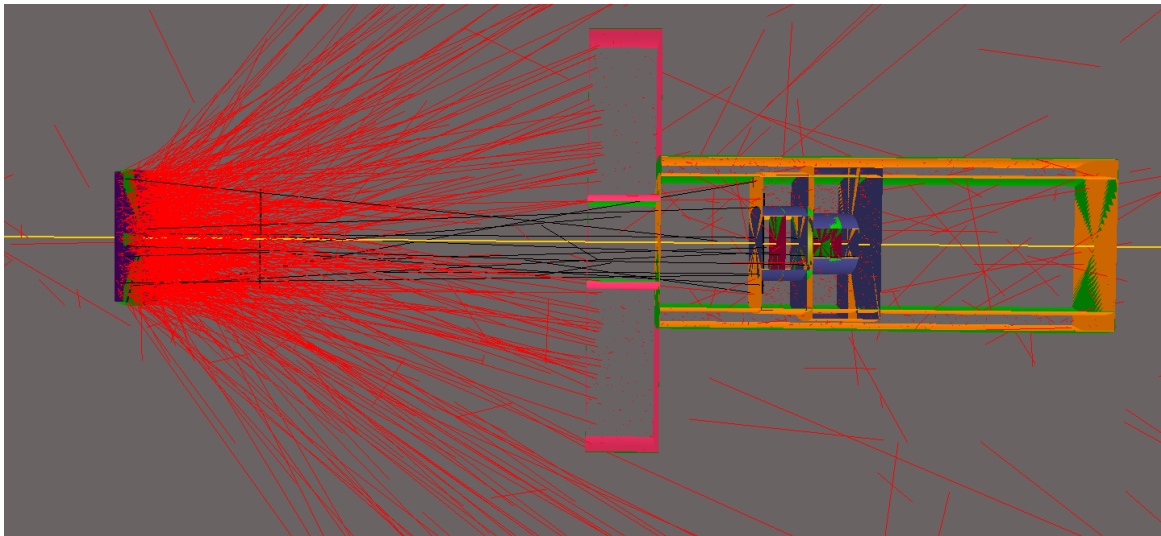


Figure 8. A visualization of the result of an MCNPX simulation of the experiment. Proton tracks (red lines) are coming from the polyethylene target (purple). Many of them strike the graphite target (pink); some of them (black lines) pass through the hole in the graphite target where they may be detected by the proton telescope (blue). The tritium target is off the page to the left.

Future Plans

Clearly, more work needs to be done before reliable cross sections spanning the energy range need for ICF diagnostics can be produced.

The uncertainty in the measurement need to be analyzed. The statistical uncertainty in the proton count rate from the proton telescope is 2-3%, so this is approximately the statistical uncertainty in the neutron flux. To determine the uncertainty in the measured cross sections the statistical uncertainty in the produced number of ^{11}C nuclei needs to be established. This uncertainty will depend upon both the count rate in each time bin and the exponential growth curve fit. The sources of systematic uncertainty must also be identified and studied. MCNPX simulations will be performed to determine the effect of source, target and detector misalignment and position uncertainty on the measured count rates.

Corrections must be calculated for the finite size of the tritium neutron source, the polyethylene target, the graphite target and the detector telescope. This will involve continuing development of an MCNPX code to accurately model the geometry of the experiment in order to account for the sizes of detectors and targets, the variation of proton and neutron cross sections and energies with angle, and the effect of these quantities on the $^{12}\text{C}(n,2n)$ reaction rate within the targets.

Cross sections for the entire tertiary neutron energy span are needed. In the past, the tandem accelerator at Ohio University has reached deuteron energies well over the design energy of 9 MeV. A deuteron energy of 9.6 MeV would produce 27 MeV neutrons. In order to reach these energies, minor modifications to the accelerator, including retracting the corona points and adding SF₆ gas will be required. Our goal for next summer will be to pursue making additional higher energy measurements of the cross section, as well as improving the measurement at lower energies. Carl Brune and Tom Massey at Ohio University have indicated their openness to consider this possibility.

Abstracts

Andrew Evans, Keith Mann and Mark Yuly. "A possible ¹²C(n,2n)¹¹C total cross section measurement." XXXI Annual Rochester Symposium for Physics Students, Siena College, Loudonville, NY, April 14, 2012; 53rd Annual Meeting of the APS Division of Plasma Physics, Salt Lake City, Utah, November 14-18, 2011.

Tertiary neutron production can be used as an indicator of the burn fraction of a deuterium-tritium pellet in inertial confinement fusion reactions. One way to monitor tertiary neutrons is by carbon activation using the ¹²C(n,2n)¹¹C reaction, which has a threshold of 20.3 MeV and so is insensitive to primary neutrons produced in the DT reaction. However, the cross section for this reaction is not well known. Several different experimental techniques for measuring ¹²C(n,2n) have been examined, with an activation experiment being the most feasible.

This material is based upon work supported by the Department of Energy [National Nuclear Security Administration] University of Rochester "National Inertial Confinement Program" under Award Number(s) DE-NA0004144.

This report was prepared as an account of work sponsored by an agency of the United States Government. Neither the United States Government nor any agency thereof, nor any of their employees, makes any warranty, express or implied, or assumes any legal liability or responsibility for the accuracy, completeness, or usefulness of any information, apparatus, product, or process disclosed, or represents that its use would not infringe privately owned rights. Reference herein to any specific commercial product, process, or service by trade name, trademark, manufacturer, or otherwise does not necessarily constitute or imply its endorsement, recommendation, or favoring by the United States Government or any agency thereof. The views and opinions of authors expressed herein do not necessarily state or reflect those of the United States Government or any agency thereof.

¹ P. J. Dimbylow, Phys. Med. Biol. **25**, 637 (1980).

² B. Anders et al., Zeit. Phys. **A 301**, 353 (1981).

³ P. Welch et al., Bull. Am. Phys. Soc. **26**, 708 (1981).

⁴ O. D. Brill et al., Dok. Akad. Nauk SSR **136**, 55 (1961); F. Nasyrov et al., At. Energ. **25**, 437 (1968).

⁵ T. S. Soewarsono et al., JAERI Tokai Rep. **27**, 354 (1992).

⁶ Uno et al., Nucl. Sci. Eng. **122**, 247 (1996); E. Kim et al., **129**, 209 (1998).

⁷ J. E. Brolley Jr. et al., Phys. Rev. **88**, 618 (1952).